
LANDMARKER: A TOOLKIT FOR ANATOMICAL LANDMARK LOCALIZATION IN 2D/3D IMAGES

A PREPRINT

 **Jef Jonkers**

IDLab

Department of Electronics and Information Systems
Ghent University, Belgium
jef.jonkers@ugent.be

 **Luc Duchateau**

Biometrics Research Group

Department of Morphology, Imaging, Orthopedics,
Rehabilitation and Nutrition
Ghent University, Belgium
luc.duchateau@ugent.be

 **Glenn Van Wallendael**

IDLab

Department of Electronics and Information Systems
Ghent University - imec, Belgium
glenn.vanwallendael@ugent.be

 **Sofie Van Hoecke**

IDLab

Department of Electronics and Information Systems
Ghent University - imec, Belgium
sofie.vanhoecke@ugent.be

January 20, 2025

ABSTRACT

Anatomical landmark localization in 2D/3D images is a critical task in medical imaging. Although many general-purpose tools exist for landmark localization in classical computer vision tasks, such as pose estimation, they lack the specialized features and modularity necessary for anatomical landmark localization applications in the medical domain. Therefore, we introduce `landmarker`, a Python package built on PyTorch. The package provides a comprehensive, flexible toolkit for developing and evaluating landmark localization algorithms, supporting a range of methodologies, including static and adaptive heatmap regression. `landmarker` enhances the accuracy of landmark identification, streamlines research and development processes, and supports various image formats and preprocessing pipelines. Its modular design allows users to customize and extend the toolkit for specific datasets and applications, accelerating innovation in medical imaging. `landmarker` addresses a critical need for precision and customization in landmark localization tasks not adequately met by existing general-purpose pose estimation tools.

Repository: <https://github.com/predict-idlab/landmarker>.

Keywords Landmark localization · Keypoint detection · Medical image analysis · Python · PyTorch

1 Motivation and significance

Landmark (or keypoint) localization in 2D/3D images is a fundamental challenge in computer vision, crucial for tasks such as pose estimation [Luvizon et al., 2018, Tompson et al., 2014, Newell et al., 2016], face alignment [Zhou et al., 2023, Kumar et al., 2019], robotic manipulation [Ziegler et al., 2020], surgical procedures [Sharan et al., 2021], and various image-based medical diagnoses [de Queiroz Tavares Borges Mesquita et al., 2023, Ryu et al., 2022, Pei et al., 2023, Payer et al., 2019, Thaler et al., 2021]. The effectiveness of different approaches is often domain and task-dependent, necessitating extensive experimentation for new applications. Popular methods, such as heatmap regression, involve numerous preprocessing and post-processing steps. The latter, such as sub-pixel accuracy methods, can significantly improve the precision needed in medical applications but nevertheless are frequently overlooked.

As existing packages such as OpenPose [Cao et al., 2021] and Ultralytics [Jocher et al., 2023] are primarily designed for pose estimation, they lack the modularity needed for medical applications. While MMPose [MMPose Contributors,

2020] offers modular components for various tasks, it is still tailored toward pose estimation and does not easily integrate with other frameworks or handle specific medical imaging requirements.

Our Python package, `landmarker`¹, addresses the need for precise anatomical landmark localization in medical images, which is critical for diagnostics and therapeutic procedures in different specialties, such as orthodontics, maxillofacial surgery, and orthopedics. It is a flexible PyTorch-based toolkit designed explicitly for anatomical landmark localization. This toolkit accelerates the development of algorithms and enhances the accuracy of landmark identification in medical images, thereby improving diagnostic and treatment outcomes. Its modular and adaptable framework allows researchers and practitioners to implement state-of-the-art algorithms tailored to their specific datasets.

`landmarker` has a modular framework, which supports various landmark localization algorithms. This flexibility enables customization and extension according to specific needs. The package offers interfaces for data preprocessing, model training, evaluation, and visualization.

2 Background: landmark localization

There are two primary methodologies in landmark localization (see Figure 1): heatmap regression and coordinate regression. Coordinate regression [Fard and Mahoor, 2022] involves learning a direct relationship between the image and the landmark locations. However, the introduction of heatmap regression [Tompson et al., 2014], which generally yields better performance, has shifted the research focus. Heatmap regression predicts a heatmap that assigns a likelihood or probability to each (down-sized) image pixel. Early heatmap regression methods, termed *direct* heatmap regression, assume a parametric distribution, typically a bivariate Gaussian or Laplacian distribution. Direct heatmap regression can be further classified into static and adaptive approaches. In static heatmap regression, the heatmap distribution parameters are fixed hyperparameters during training. In adaptive heatmap regression, these parameters are adjusted during training, either by treating them as learnable model parameters [Payer et al., 2019, 2020, Thaler et al., 2021] or by using scheduling methods that modify the parameters based on specific evaluation metrics [Teixeira et al., 2019]. Another variant of static heatmap regression involves training a model on one-hot heatmap images (masks), essentially parameterizing the heatmap as a categorical distribution and transforming the task into a multi-class classification problem where each pixel represents a class [McCout and Voiculescu, 2022].

Recent advancements on heatmap regression have seen the rise of fully convolutional neural networks (CNNs) with differentiable decoding operations, such as the soft-argmax operation [Luvizon et al., 2018]. These methods, prominent in facial landmark localization, use the heatmap generation layer as an intermediate layer and the decoding operation as the final layer, optimizing the network with a loss function that compares the decoded coordinates to the ground-truth coordinates. Some of these methods account for the ambiguity in landmark ground truth by incorporating uncertainty-aware loss functions, such as the Gaussian log-likelihood loss [Kumar et al., 2019], or other custom loss functions [Kumar et al., 2019, 2020, Zhou et al., 2023].

In the medical domain, landmark localization often employs two-stage approaches [Jiang et al., 2022, Song et al., 2020, Zhong et al., 2019]. The first stage localizes landmarks on a low-resolution image, and the second stage refines this localization on a high-resolution patch, which is a region of interest based on the initial predictions. In both stages, one of the previously described approaches can be used.

The diversity of approaches in landmark localization, from basic coordinate regression to sophisticated uncertainty-aware heatmap methods, highlights the complexity of this field, particularly in medical imaging applications. While general-purpose tools like OpenPose and MMPose exist, they primarily focus on human pose estimation and lack the specialized features needed for medical imaging applications. These tools often do not support the full range of heatmap

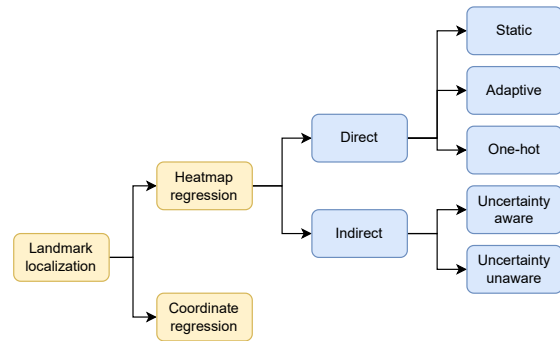


Figure 1: Taxonomy of (deep learning) landmark localization approaches. The frequently used taxonomy in the literature is highlighted in yellow, while our extended taxonomy of the problem is highlighted in blue.

¹<https://github.com/predict-idlab/landmarker>

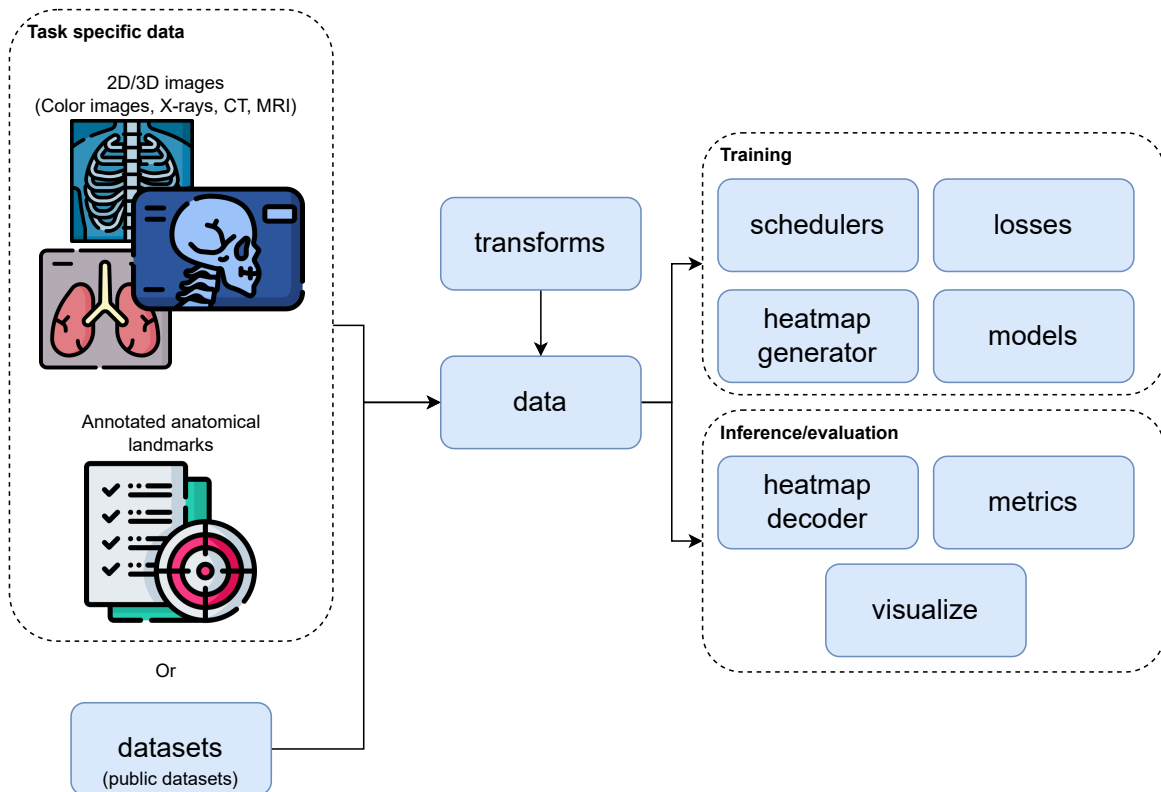


Figure 2: Flowchart of the different sub-packages of the `landmarker` package.

generation and decoding methods, uncertainty quantification, or medical image-specific preprocessing pipelines crucial for anatomical landmark localization. Additionally, existing tools typically do not provide the modularity required to implement and experiment with different approaches, such as two-stage refinement methods commonly used in medical applications. These limitations, combined with the need for high precision in medical contexts, underscore the need for a specialized toolkit to handle the unique challenges of anatomical landmark localization while supporting established and emerging methodologies.

3 Software description

`landmarker` is a Python package that leverages PyTorch [Paszke et al., 2019] deep learning framework and MONAI [Cardoso et al., 2022], a PyTorch-based deep learning framework for healthcare imaging for handling medical image files and transformations.

Users can install `landmarker` via `pip`. After installation, our documentation and variety of examples will guide users in applying the toolkit for their specific needs.

3.1 Software architecture and functionalities

The `landmarker` package is structured into several key modules, each addressing specific aspects of the landmark localization pipeline, see Figure 2.

3.1.1 Data handling and preprocessing

The `data` module provides flexible *"dataset"* classes that inherit from PyTorch's `Dataset`, ensuring compatibility with PyTorch `DataLoaders`. Four main dataset types are supported:

- `LandmarkDataset`: For images with corresponding landmark coordinates.
- `HeatmapDataset`: For images with corresponding static heatmaps representing landmarks.
- `MaskDataset`: For images with binary segmentation masks indicating landmark locations.
- `PatchDataset`: For image patches or regions of interest (ROI) with corresponding landmarks.

These datasets support various image formats (NIfTI, DICOM, PNG, JPG, BMP, NPY/NPZ) through integration with the MONAI library [Cardoso et al., 2022]. The module can handle single-class, multi-class single-instance, and multi-class multi-instance landmark problems. Utility functions are provided to transform common annotation formats (e.g., labelme [Wada, 2024]) into the required format.

The package also includes the `datasets` module, which contains functions to import benchmark datasets, such as the ISBI2015 [Wang et al., 2016] dataset directly. Preprocessing and data augmentation capabilities are available, leveraging MONAI’s transformations for 2D and 3D data. The package handles affine landmarks transformations through the `transforms` module.

3.1.2 Heatmap generation and decoding

The heatmap module provides functionality for generating target heatmaps and decoding predicted heatmaps, which is essential for heatmap regression approaches.

3.1.2.1 Heatmap generation

The `HeatmapGenerator` class and its subclasses support various parametric distributions (e.g., multivariate Gaussian and Laplace). The design allows easy implementation of custom distributions. The parameters of the parametric distribution can be set on initialization. Still, they can also be changed during training, for example, for adaptive heatmap regression approaches that rely on a scheduler, such as Adaloss scheduler [Teixeira et al., 2019]. Additionally, the parameters could also be learnable parameters during a training procedure.

3.1.2.2 Heatmap decoding

While heatmap generation is only needed for direct approaches, decoding heatmaps is needed for all heatmap regression approaches, with the caveat that the indirect approaches need differentiable decoding operations. Multiple decoding methods are implemented:

The *argmax* operation is the simplest decoder operation [Tompson et al., 2014]. The operation takes the maximum value of the heatmap H_i ,

$$\hat{y}_i = \operatorname{argmax} H_i, \quad (1)$$

to get the coordinate \hat{y}_i of landmark i . The major downside of this approach is that it introduces a discretization error by only choosing a pixel as the predicted landmark.

The *weighted spatial mean* [Luvizon et al., 2018, Dong et al., 2018, Kumar et al., 2019, 2020] is the approach for indirect heatmap generation. The operation calculates the landmark location \hat{y}_i by first post-processing the heatmap H_i with an activation function σ , typically a type of normalization operation, and afterward taking the weighted spatial mean, e.g., the two-dimensional case:

$$\hat{y}_i = \left(\sum_{c=0}^W \sum_{l=0}^H \frac{c}{W} \sigma(H_i)_{l,c}, \sum_{c=0}^W \sum_{l=0}^H \frac{l}{H} \sigma(H_i)_{l,c} \right) \quad (2)$$

where W and H are, respectively, the heatmap’s width and height. Frequently used activation functions σ are a ReLU activation combined with a normalization procedure and the softmax operation on the heatmap, which is in the literature often referred to as soft-argmax operation [Luvizon et al., 2018, Dong et al., 2018, Bulat et al., 2021].

A significant issue of taking the weighted spatial mean is that it can globally lead to semantically unstructured outputs and thus decrease performance [Bulat et al., 2021]. In Bulat et al. [2021], they propose to apply soft-argmax operation locally, i.e., a small window, around the heatmap location with a maximum heatmap value. We implement this method and extend it to be used with any post-processing function, i.e., *local weight spatial mean* operation.

3.1.3 Models and losses

While `landmarker` is compatible with any PyTorch model or loss function, it includes implementations of successful approaches from the literature, such as the spatial configuration network [Payer et al., 2019], which is effective for positionally consistent medical images like cephalograms. Also, multiple heatmap regression loss functions are implemented from successful approaches [Thaler et al., 2021, Nibali et al., 2018, Kumar et al., 2019, Feng et al., 2018, Wang et al., 2019, Zhou et al., 2023].

3.1.4 Evaluation and visualization

The `visualize` module allows inspecting constructed datasets and trained models. Additionally, it enables the generation of detection reports that output several metrics from the `metrics` module, such as point error and success detection rate (SDR), which is the percentage of predicted landmarks with a point error smaller or equal to a specified radius.

4 Illustrative examples

In this section, we illustrate the use of `landmarker`. We will perform adaptive heatmap regression with the ISBI2015 cephalometric landmark dataset, showcasing most functionality.

We start by loading the data into a `LandmarkDataset` by providing a list of paths to images, a NumPy array of the shape (N, C, D) where N is the number of samples, C is the number of landmark classes, and D represents the spatial dimension which can be 2 or 3.

```

1 from landmarker.data import LandmarkDataset
2
3 image_paths = ... # list of paths of images
4 landmarks = ... # numpy array or torch tensor provided
5 pixel_spacing = ... # pixel spacing of the images
6 class_names = ... # names of the landmarks
7 compose_transform = ... # MONAI compose transform
8
9 ds = LandmarkDataset(
10     imgs=image_paths,
11     landmarks=landmarks,
12     spatial_dims=2,
13     transform=compose_transform,
14     dim_img=(512,512) # dimension to resize to
15     class_names=class_names)

```

Listing 1: Loading data into a `LandmarkDataset`

Alternatively, one can also use the dataset module, which includes everything to import the ISBI2015 dataset directly.

```

1 from landmarker.dataset import get_cepha_landmark_datasets
2
3 data_dir = ...
4 ds_train, ds_test1, ds_test2 = get_cepha_landmark_datasets(data_dir)

```

Listing 2: Loading data into a `LandmarkDataset` through the dataset module.

Once the data is loaded in the proper format, we can set up the heatmap generator to generate a heatmap from landmarks.

```

1 from landmarker.heatmap import GaussianHeatmapGenerator
2
3 generator = GaussianHeatmapGenerator(
4     nb_landmarks=19, # number of landmarks
5     sigmas=3, # sd. value of the Gaussian heatmap function
6     learnable=True, # make the covariance matrix learnable parameters
7     heatmap_size=(512,512))

```

Listing 3: Setting up Gaussian heatmap generator.

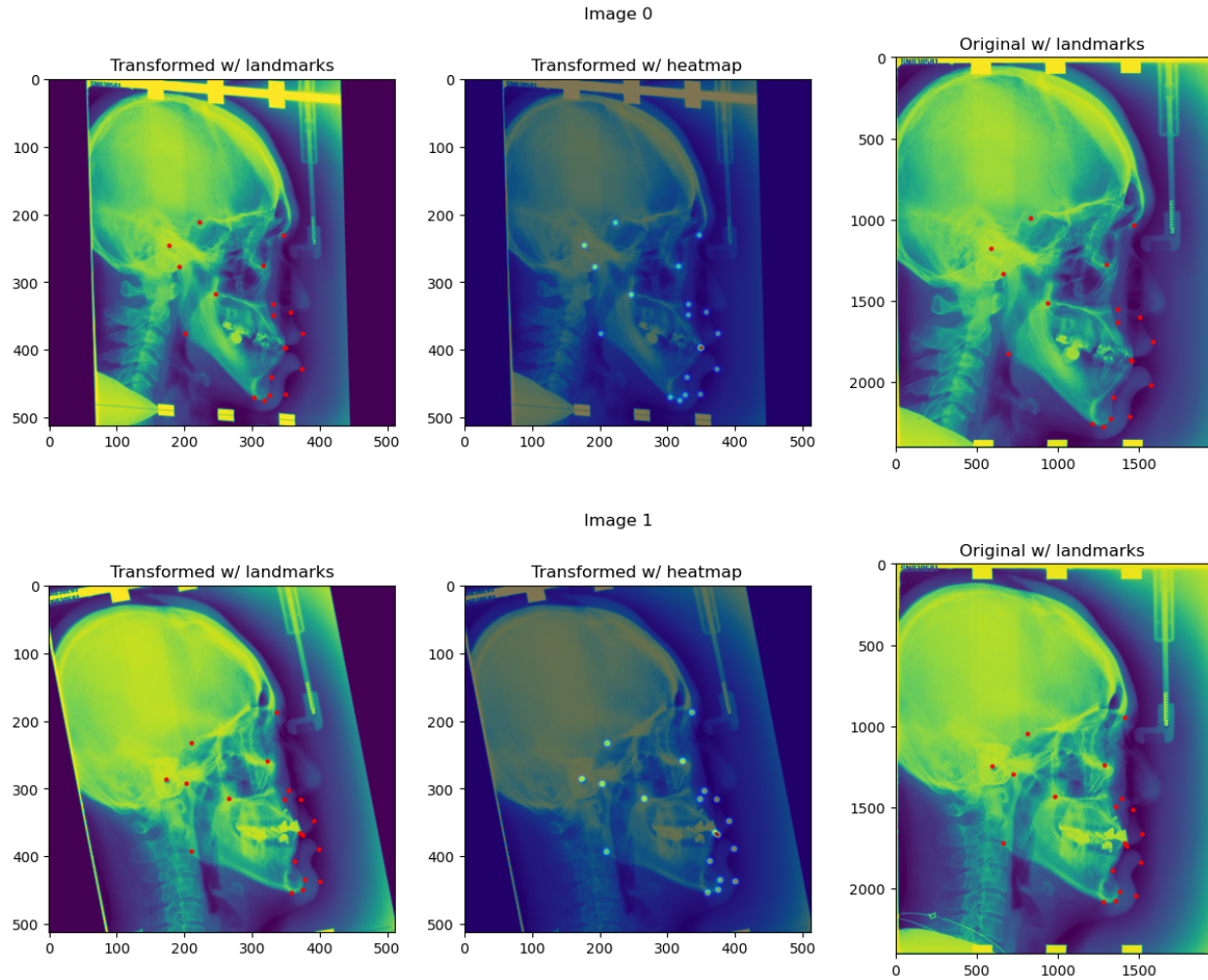


Figure 3: Example of results of running the `inspection_plot` on the ISBI2015 dataset.

After this, the user can visually inspect if everything is initialized as expected by using the `inspection_plot` function (Listing 4 and Figure 3).

```

1 from landmarker.visualize import inspection_plot
2
3 inspection_plot(ds_train, range(3), heatmap_generator=heatmap_generator)

```

Listing 4: Loading data into a LandmarkDataset

With the LandmarkDataset and HeatmapGenerator adequately set up, we can now train a model to output likelihood heatmaps. In Listing 5, we train a SpatialConfigurationNetwork [Payer et al., 2019, Thaler et al., 2021] and parameterization of the Gaussian heatmap [Payer et al., 2020, Thaler et al., 2021].

```

1 import torch
2
3 from landmarker.models import OriginalSpatialConfigurationNet
4 from landmarker.losses import GaussianHeatmapL2Loss
5
6 model = OriginalSpatialConfigurationNet(in_channels=1, out_channels=19)
7 optimizer = torch.optim.SGD([
8     {'params': model.parameters(), "weight_decay": 1e-3},
9     {'params': heatmap_generator.sigmas},

```

```
10 {'params': heatmap_generator.rotation}}
11 , lr=1e-6, momentum=0.99, nesterov=True)
12
13 criterion = GaussianHeatmapL2Loss(alpha=5)
14
15 train_loader = DataLoader(ds_train, batch_size=1, shuffle=True, num_workers=0)
16
17 # Start training
18 for epoch in range(100):
19     model.train()
20     for batch in train_loader:
21         images = batch["image"].to(device)
22         landmarks = batch["landmark"].to(device)
23         optimizer.zero_grad()
24         outputs = model(images)
25         heatmaps = heatmap_generator(landmarks)
26         loss = criterion(outputs, heatmap_generator.sigmas, heatmaps)
27         loss.backward()
28         optimizer.step()
```

Listing 5: Training adaptive heatmap regression model.

After the training procedure, one can visually evaluate the results by using the `prediction_inspect_plot` function (see Listing 6 and Figure 4) or by creating a detection report.

```
1 from landmarker.visualize import prediction_inspect_plot
2
3 prediction_inspect_plot(ds_test1, model, ds_test1.indices[:3])
```

Listing 6: Prediction inspection plot.

5 Impact and conclusions

The development and release of the `landmarker` Python package offer significant advancements in anatomical landmark localization, particularly within medical imaging. By providing a flexible and modular toolkit tailored explicitly for medical imaging applications, `landmarker` addresses a critical need for precision and customization in landmark localization tasks that are not adequately met by existing general-purpose pose estimation tools like OpenPose or MMPose.

One of the key impacts of `landmarker` is its ability to streamline the research and development process for researchers and developers working on image-based diagnostic and therapeutic deep learning applications. The package’s integration with PyTorch and MONAI ensures compatibility with various medical image formats and processing pipelines, facilitating easy adoption in research environments. Moreover, the extensive support for different landmark localization methodologies, including static and adaptive heatmap regression, allows users to implement state-of-the-art algorithms with minimal overhead.

Including customizable modules for data handling, preprocessing, heatmap generation, and model evaluation further enhances the utility of `landmarker`. These features enable users to quickly adapt the package to their specific use cases, whether they involve 2D or 3D images, single-class or multi-class landmark localization, or static versus adaptive methodologies. The ability to implement and test novel approaches within a unified framework accelerates innovation in computer-aided diagnosis through medical imaging, potentially leading to more accurate diagnoses and better patient outcomes.

In conclusion, `landmarker` represents a powerful tool for advancing the field of anatomical landmark localization in medical imaging. Its flexibility and ease of use make it a helpful resource for researchers and engineers.

Funding sources

Jef Jonkers is funded by the Research Foundation Flanders (FWO, Ref. 1S11525N).

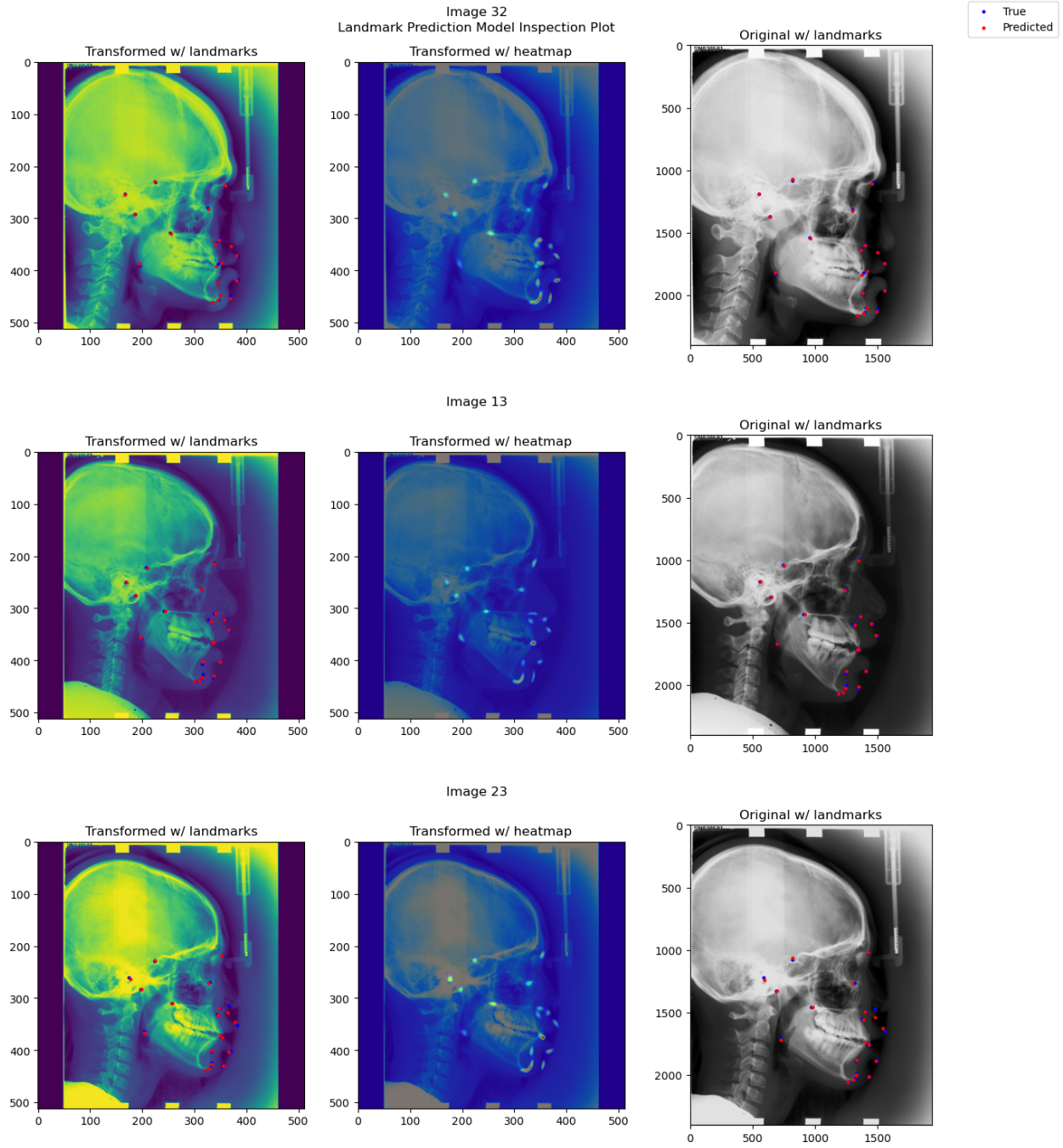


Figure 4: Example of results of running the prediction_inspection_plot on the ISBI2015 dataset.

References

- Diogo C. Luvizon, David Picard, and Hedi Tabia. 2D/3D Pose Estimation and Action Recognition using Multitask Deep Learning, March 2018. URL <http://arxiv.org/abs/1802.09232>. arXiv:1802.09232 [cs].
- Jonathan J Tompson, Arjun Jain, Yann LeCun, and Christoph Bregler. Joint Training of a Convolutional Network and a Graphical Model for Human Pose Estimation. In *Advances in Neural Information Processing Systems*, volume 27. Curran Associates, Inc., 2014. URL <https://proceedings.neurips.cc/paper/2014/hash/e744f91c29ec99f0e662c9177946c627-Abstract.html>.
- Alejandro Newell, Kaiyu Yang, and Jia Deng. Stacked Hourglass Networks for Human Pose Estimation. In Bastian Leibe, Jiri Matas, Nicu Sebe, and Max Welling, editors, *Computer Vision – ECCV 2016*, Lecture Notes in Computer Science, pages 483–499, Cham, 2016. Springer International Publishing. ISBN 978-3-319-46484-8. doi:10.1007/978-3-319-46484-8_29.
- Zhenglin Zhou, Huaxia Li, Hong Liu, Nanyang Wang, Gang Yu, and Rongrong Ji. STAR Loss: Reducing Semantic Ambiguity in Facial Landmark Detection. In *Proceedings of the IEEE/CVF Conference on Computer Vision and Pattern Recognition*, pages 15475–15484, 2023. URL https://openaccess.thecvf.com/content/CVPR2023/html/Zhou_STAR_Loss_Reducing_Semantic_Ambiguity_in_Facial_Landmark_Detection_CVPR_2023_paper.html.
- Abhinav Kumar, Tim K. Marks, Wenxuan Mou, Chen Feng, and Xiaoming Liu. UGLLI Face Alignment: Estimating Uncertainty with Gaussian Log-Likelihood Loss. In *2019 IEEE/CVF International Conference on Computer Vision Workshop (ICCVW)*, pages 778–782, Seoul, Korea (South), October 2019. IEEE. ISBN 978-1-72815-023-9. doi:10.1109/ICCVW.2019.00103. URL <https://ieeexplore.ieee.org/document/9022191/>.
- Thomas Ziegler, Judith Butepage, Michael C. Welle, Anastasiia Varava, Tonci Novkovic, and Danica Kragic. Fashion Landmark Detection and Category Classification for Robotics, March 2020. URL <http://arxiv.org/abs/2003.11827>. arXiv:2003.11827 [cs, stat].
- Lalith Sharan, Gabriele Romano, Julian Brand, Halvar Kelm, Matthias Karck, Raffaele De Simone, and Sandy Engelhardt. Point detection through multi-instance deep heatmap regression for sutures in endoscopy. *International Journal of Computer Assisted Radiology and Surgery*, 16(12):2107–2117, December 2021. ISSN 1861-6429. doi:10.1007/s11548-021-02523-w. URL <https://doi.org/10.1007/s11548-021-02523-w>.
- Germana de Queiroz Tavares Borges Mesquita, Walbert A. Vieira, Maria Tereza Campos Vidigal, Bruno Augusto Nassif Travençolo, Thiago Leite Beaini, Rubens Spin-Neto, Luiz Renato Paranhos, and Rui Barbosa de Brito Júnior. Artificial Intelligence for Detecting Cephalometric Landmarks: A Systematic Review and Meta-analysis. *Journal of Digital Imaging*, January 2023. ISSN 1618-727X. doi:10.1007/s10278-022-00766-w. URL <https://doi.org/10.1007/s10278-022-00766-w>.
- Seung Min Ryu, Keewon Shin, Soo Wung Shin, Sun Ho Lee, Su Min Seo, Seung-uk Cheon, Seung-Ah Ryu, Jun-Sik Kim, Sunghwan Ji, and Namkug Kim. Automated landmark identification for diagnosis of the deformity using a cascade convolutional neural network (FlatNet) on weight-bearing lateral radiographs of the foot. *Computers in Biology and Medicine*, 148:105914, September 2022. ISSN 0010-4825. doi:10.1016/j.combiomed.2022.105914. URL <https://www.sciencedirect.com/science/article/pii/S0010482522006576>.
- Yun Pei, Lin Mu, Chuanxin Xu, Qiang Li, Gan Sen, Bin Sun, Xiuying Li, and Xueyan Li. Learning-based landmark detection in pelvis x-rays with attention mechanism: data from the osteoarthritis initiative. *Biomedical Physics & Engineering Express*, 9(2):025001, January 2023. ISSN 2057-1976. doi:10.1088/2057-1976/ac8ffa. URL <https://dx.doi.org/10.1088/2057-1976/ac8ffa>.
- Christian Payer, Darko Stern, Horst Bischof, and Martin Urschler. Integrating spatial configuration into heatmap regression based CNNs for landmark localization. *Medical Image Analysis*, 54:207–219, May 2019. ISSN 1361-8415. doi:10.1016/j.media.2019.03.007. URL <https://www.sciencedirect.com/science/article/pii/S1361841518305784>.
- Franz Thaler, Christian Payer, Martin Urschler, and Darko Stern. Modeling Annotation Uncertainty with Gaussian Heatmaps in Landmark Localization, September 2021. URL <http://arxiv.org/abs/2109.09533>. arXiv:2109.09533 [cs].
- Zhe Cao, Gines Hidalgo, Tomas Simon, Shih-En Wei, and Yaser Sheikh. OpenPose: Realtime Multi-Person 2D Pose Estimation Using Part Affinity Fields. *IEEE Transactions on Pattern Analysis and Machine Intelligence*, 43(1): 172–186, January 2021. ISSN 1939-3539. doi:10.1109/TPAMI.2019.2929257. URL <https://ieeexplore.ieee.org/document/8765346>. Conference Name: IEEE Transactions on Pattern Analysis and Machine Intelligence.
- Glenn Jocher, Jing Qiu, and Ayush Chaurasia. Ultralytics YOLO, January 2023. URL <https://github.com/ultralytics/ultralytics>. original-date: 2022-09-11T16:39:45Z.

- MMPose Contributors. OpenMMLab Pose Estimation Toolbox and Benchmark, August 2020. URL <https://github.com/open-mmlab/mmpose>. original-date: 2020-07-08T06:02:55Z.
- Ali Pourramezan Fard and Mohammah H. Mahoor. ACR Loss: Adaptive Coordinate-based Regression Loss for Face Alignment. In *2022 26th International Conference on Pattern Recognition (ICPR)*, pages 1807–1814, August 2022. doi:10.1109/ICPR56361.2022.9956683. ISSN: 2831-7475.
- Christian Payer, Martin Urschler, Horst Bischof, and Darko Štern. Uncertainty Estimation in Landmark Localization Based on Gaussian Heatmaps. In Carole H. Sudre, Hamid Fehri, Tal Arbel, Christian F. Baumgartner, Adrian Dalca, Ryutaro Tanno, Koen Van Leemput, William M. Wells, Aristeidis Sotiras, Bartłomiej Papież, Enzo Ferrante, and Sarah Parisot, editors, *Uncertainty for Safe Utilization of Machine Learning in Medical Imaging, and Graphs in Biomedical Image Analysis*, Lecture Notes in Computer Science, pages 42–51, Cham, 2020. Springer International Publishing. ISBN 978-3-030-60365-6. doi:10.1007/978-3-030-60365-6_5.
- Brian Teixeira, Birgi Tamersoy, Vivek Singh, and Ankur Kapoor. Adaloss: Adaptive Loss Function for Landmark Localization, August 2019. URL <http://arxiv.org/abs/1908.01070>. arXiv:1908.01070 [cs].
- James McCouat and Irina Voiculescu. Contour-Hugging Heatmaps for Landmark Detection. In *2022 IEEE/CVF Conference on Computer Vision and Pattern Recognition (CVPR)*, pages 20565–20573, June 2022. doi:10.1109/CVPR52688.2022.01994. URL <https://ieeexplore.ieee.org/document/9879107>. ISSN: 2575-7075.
- Abhinav Kumar, Tim K. Marks, Wenxuan Mou, Ye Wang, Michael Jones, Anoop Cherian, Toshiaki Koike-Akino, Xiaoming Liu, and Chen Feng. LUVLi Face Alignment: Estimating Landmarks’ Location, Uncertainty, and Visibility Likelihood. In *Proceedings of the IEEE/CVF Conference on Computer Vision and Pattern Recognition*, pages 8236–8246, 2020. URL https://openaccess.thecvf.com/content_CVPR_2020/html/Kumar_LUVLi_Face_Alignment_Estimating_Landmarks_Location_Uncertainty_and_Visibility_Likelihood_CVPR_2020_paper.html.
- Yankai Jiang, Yiming Li, Xinyue Wang, Yubo Tao, Jun Lin, and Hai Lin. CephalFormer: Incorporating Global Structure Constraint into Visual Features for General Cephalometric Landmark Detection. In Linwei Wang, Qi Dou, P. Thomas Fletcher, Stefanie Speidel, and Shuo Li, editors, *Medical Image Computing and Computer Assisted Intervention – MICCAI 2022*, Lecture Notes in Computer Science, pages 227–237, Cham, 2022. Springer Nature Switzerland. ISBN 978-3-031-16437-8. doi:10.1007/978-3-031-16437-8_22.
- Yu Song, Xu Qiao, Yutaro Iwamoto, and Yen-wei Chen. Automatic Cephalometric Landmark Detection on X-ray Images Using a Deep-Learning Method. *Applied Sciences*, 10(7):2547, January 2020. ISSN 2076-3417. doi:10.3390/app10072547. URL <https://www.mdpi.com/2076-3417/10/7/2547>. Number: 7 Publisher: Multidisciplinary Digital Publishing Institute.
- Zhusi Zhong, Jie Li, Zhenxi Zhang, Zhicheng Jiao, and Xinbo Gao. An Attention-Guided Deep Regression Model for Landmark Detection in Cephalograms. In Dinggang Shen, Tianming Liu, Terry M. Peters, Lawrence H. Staib, Caroline Essert, Sean Zhou, Pew-Thian Yap, and Ali Khan, editors, *Medical Image Computing and Computer Assisted Intervention – MICCAI 2019*, Lecture Notes in Computer Science, pages 540–548, Cham, 2019. Springer International Publishing. ISBN 978-3-030-32226-7. doi:10.1007/978-3-030-32226-7_60.
- Adam Paszke, Sam Gross, Francisco Massa, Adam Lerer, James Bradbury, Gregory Chanan, Trevor Killeen, Zeming Lin, Natalia Gimelshein, Luca Antiga, Alban Desmaison, Andreas Köpf, Edward Yang, Zach DeVito, Martin Raison, Alykhan Tejani, Sasank Chilamkurthy, Benoit Steiner, Lu Fang, Junjie Bai, and Soumith Chintala. PyTorch: An Imperative Style, High-Performance Deep Learning Library, December 2019. URL <http://arxiv.org/abs/1912.01703>. arXiv:1912.01703 [cs, stat].
- M. Jorge Cardoso, Wenqi Li, Richard Brown, Nic Ma, Eric Kerfoot, Yiheng Wang, Benjamin Murrey, Andriy Myronenko, Can Zhao, Dong Yang, Vishwesh Nath, Yufan He, Ziyue Xu, Ali Hatamizadeh, Andriy Myronenko, Wentao Zhu, Yun Liu, Mingxin Zheng, Yucheng Tang, Isaac Yang, Michael Zephyr, Behrooz Hashemian, Sachidanand Alle, Mohammad Zalbagi Darestani, Charlie Budd, Marc Modat, Tom Vercauteren, Guotai Wang, Yiwen Li, Yipeng Hu, Yunguan Fu, Benjamin Gorman, Hans Johnson, Brad Genereaux, Barbaros S. Erdal, Vikash Gupta, Andres Diaz-Pinto, Andre Dourson, Lena Maier-Hein, Paul F. Jaeger, Michael Baumgartner, Jayashree Kalpathy-Cramer, Mona Flores, Justin Kirby, Lee A. D. Cooper, Holger R. Roth, Daguang Xu, David Bericat, Ralf Floca, S. Kevin Zhou, Haris Shuaib, Keyvan Farahani, Klaus H. Maier-Hein, Stephen Aylward, Prerna Dogra, Sebastien Ourselin, and Andrew Feng. MONAI: An open-source framework for deep learning in healthcare, November 2022. URL <http://arxiv.org/abs/2211.02701>. arXiv:2211.02701 [cs].
- Kentaro Wada. Labelme: Image Polygonal Annotation with Python, August 2024. URL <https://github.com/wkentaro/labelme>.

- Ching-Wei Wang, Cheng-Ta Huang, Jia-Hong Lee, Chung-Hsing Li, Sheng-Wei Chang, Ming-Jhih Siao, Tat-Ming Lai, Bulat Ibragimov, Tomaž Vrtovec, Olaf Ronneberger, Philipp Fischer, Tim F. Cootes, and Claudia Lindner. A benchmark for comparison of dental radiography analysis algorithms. *Medical Image Analysis*, 31:63–76, July 2016. ISSN 1361-8415. doi:10.1016/j.media.2016.02.004. URL <https://www.sciencedirect.com/science/article/pii/S1361841516000190>.
- Xuanyi Dong, Shoou-I. Yu, Xinshuo Weng, Shih-En Wei, Yi Yang, and Yaser Sheikh. Supervision-by-Registration: An Unsupervised Approach to Improve the Precision of Facial Landmark Detectors. pages 360–368, 2018. URL https://openaccess.thecvf.com/content_cvpr_2018/html/Dong_Supervision-by-Registration_An_Unsupervised_CVPR_2018_paper.html.
- Adrian Bulat, Enrique Sanchez, and Georgios Tzimiropoulos. Subpixel Heatmap Regression for Facial Landmark Localization, November 2021. URL <http://arxiv.org/abs/2111.02360>. arXiv:2111.02360 [cs].
- Aiden Nibali, Zhen He, Stuart Morgan, and Luke Prendergast. Numerical Coordinate Regression with Convolutional Neural Networks, May 2018. URL <http://arxiv.org/abs/1801.07372>. arXiv:1801.07372 [cs].
- Zhen-Hua Feng, Josef Kittler, Muhammad Awais, Patrik Huber, and Xiao-Jun Wu. Wing Loss for Robust Facial Landmark Localisation With Convolutional Neural Networks. pages 2235–2245, 2018. URL https://openaccess.thecvf.com/content_cvpr_2018/html/Feng_Wing_Loss_for_CVPR_2018_paper.html.
- Xinyao Wang, Liefeng Bo, and Li Fuxin. Adaptive Wing Loss for Robust Face Alignment via Heatmap Regression. pages 6971–6981, 2019. URL https://openaccess.thecvf.com/content_ICCV_2019/html/Wang_Adaptive_Wing_Loss_for_Robust_Face_Alignment_via_Heatmap_Regression_ICCV_2019_paper.html.